Inorg. Chem. **2006**, *45*, 5878–5885

Ag_3SnCuP_{10}: [Ag_3Sn] Tetrahedra Embedded between Adamantane-Type [P_{10}] Cages

Stefan Lange,[†] C. Peter Sebastian,[†] Long Zhang,[‡] Hellmut Eckert,[‡] and Tom Nilges*[,†]

Institute of Inorganic and Analytical Chemistry and Institute of Physical Chemistry, University of Münster, Corrensstrasse 30, 48149 Münster, Germany

Received March 7, 2006

Ag_3SnCuP_{10} was synthesized from a stoichiometric mixture of copper, silver, tin, and red phosphorus, with SnI_4 added as a mineralization agent. Cubic Ag_3SnCuP_{10}, space group $F\bar{4}3m$ (No. 216) with lattice parameter $a = 10.503(1)$ Å and $Z = 4$, consisting of orientationally disordered [Ag_3Sn] heteroclusters and adamantane-type [P_{10}] cages, is one example in which structure determination was possible only by the combined use of diffraction and spectroscopic methods. An ideal 4-fold domain twin structure that results for a $R3m$ model, featuring an ordered arrangement of the heteroclusters, cannot be differentiated from the $F\bar{4}3m$ model by diffraction methods alone. After a detailed NMR spectroscopic examination using state of the art solid-state NMR techniques, we found the local environment around the [P_{10}] cages of the $F\bar{4}3m$ model to be the correct description of the Ag_3SnCuP_{10} structure. A possible Cu/Ag or Ag/Sn disorder in the [Ag_3Sn] heterocluster and within the copper substructure was excluded by Mössbauer spectroscopic investigations and NMR measurements.

Introduction

For more than 40 years, the preparation and characterization of phosphides has resulted in a plethora of materials that feature an intriguing variety of compositions and structures.[1,2] Among the numerous P_n structural motifs realized, the adamantane-like $[P_{10}]^{6-}$ cage has been observed in only one compound to date.[3,4] Cu_4SnP_{10} ($a = 10.267(1)$ Å, space group $F\bar{4}3m$, No. 216) belongs to the family of ternary diamond-related structures. The latter can be derived from the sphalerite structure that shows four defects at the centers of the [Cu_3Sn] tetrahedra, which are embedded in the phosphorus substructure. Band-structure calculations reveal the interesting bonding situation of the two-electron, four-center cluster.[5] Tin atoms are coordinated trigonal-antiprismatically by three phosphorus and three copper atoms. Only a small proportion of sp^3 hybridization is present in the pseudotetrahedral tin environment formed by three P ligands and a free lone pair pointing toward the copper atoms. Bonding in the [Cu_3Sn] cluster is therefore dominated by s orbital contributions. Copper and tin atoms are disordered to form a closely neighbored split position caused by a statistical orientation of [Cu_3Sn] tetrahedra. In addition, large displacement parameters suggest a high atomic mobility, at least in the [Cu_3Sn] cluster; however, this feature has not been studied in detail.

Recently, a novel heterocluster has been reported in Ag_3SnP_7 that features $^1_\infty[P_7]$ chains interconnected by [Ag_3Sn] units.[6] Molecular-orbital calculations at the extended Hückel level reveal that the electronic structures of the [Ag_3Sn] cluster in this compound and the [Cu_3Sn] cluster in Cu_4SnP_{10} are rather similar. Most recently, the structural motif of a tetrahedral transition/post-transition metal cluster [Ag_3Hg] and a comparable electronic structure have been reported to occur in the mineral tillmannsite.[7]

In the past few years, an ongoing scientific interest has emerged to develop new crystalline or amorphous materials with the aim of substituting the graphite anode in battery

* To whom correspondence should be addressed. Phone: 49-251-83-36645. Fax: 49-251-83-36002. E-mail: nilges@uni-muenster.de.
† Institute of Inorganic and Analytical Chemistry.
‡ Institute of Physical Chemistry.

(1) von Schnering, H. G. *Chem. Rev.* **1988**, *88*, 243−273.
(2) (a) Pöttgen, R.; Hönle, W.; von Schnering, H. G. *Encyclopedia of Inorganic Chemistry*, 2nd ed.; King, R. B., Ed.; Wiley: Chichester, U.K., 2005; Vol. VIII, pp 4255−4308. (b) Kanatzidis, M. G.; Pöttgen, R.; Jeitschko, W. *Angew. Chem.* **2005**, *117*, 7156−7184; *Angew. Chem., Int. Ed.* **2005**, *44*, 6996−7023.
(3) Goryunova, N. A.; Orlov, V. M.; Sokolova, V. I.; Shepenkov, G. P.; Tsvetkova, E. V. *Phys. Status Solidi* A **1970**, *3*, 75−87.
(4) Hönle, W.; von Schnering, H. G. *Z. Kristallogr.* **1980**, *153*, 339−350.
(5) Bullet, D. W.; Dawson, W. G. *Solid State Commun.* **1986**, *60*, 767−769.
(6) Shatruk, M. M.; Kovnir, K. A.; Shevelkov, A. V.; Popovkin, B. A. *Angew. Chem.* **2000**, *112*, 2561−2562; *Angew. Chem., Int. Ed.* **2000**, *39*, 2508−2509.
(7) (a) Sarp, H.; Pushcharovsky, D. Y.; MacLean, E. J.; Teat, S. J.; Zubkova, N. V. *Eur. J. Mineral.* **2003**, *15*, 177−180. (b) Weil, M.; Tillmanns, E.; Pushcharovsky, D. Y. *Inorg. Chem.* **2005**, *44*, 1443−1451.

10.1021/ic060380a CCC: $33.50
Published on Web 06/21/2006

systems and developing new ion conductors for use as nonvolatile memory devices. Potential candidates for anode materials in rechargeable batteries such as Zn_3P_2,[8] $CuSn_{0.88}$−CuSn,[9] or amorphous SnO,[10] for instance, are showing promising electronic properties but limited capacity retention tendencies. Amorphous and crystalline silver compounds are used for the fabrication of so-called programmable metallization cell memory devices (PMC). Nanosized metal spots are generated by an electrochemical process in thin films of solid silver electrolytes.[11] Recently, we started to work on copper- and silver-containing polyphosphides, trying to find promising new candidates that contribute to one or both of the above-mentioned topics.

The postulated mobility of copper in Cu_4SnP_{10} inspired us to have a closer look at the structural properties and ion dynamics of Cu_4SnP_{10} and encouraged us to extend our work to other potentially mobile ions such as silver and lithium. A high ion mobility plays a key role in an efficient ion intercalation/deintercalation process and should be addressed before further electrochemical experiments are performed. Unfortunately, we have not been able to prepare lithium-containing materials so far, but we succeeded in the partial exchange of copper by silver to form Ag_3SnCuP_{10}.

Experimental Section

Synthesis. SnI_4 was prepared by mixing tin (12 g, 0.10 mole) and iodine (40 g, 0.16 mole) in toluene (250 mL).[12] The mixture was refluxed for approximately 30 min until the violet color of iodine disappeared. The hot solution was decanted from the remaining tin. Orange SnI_4 crystallized after cooling to room temperature. The crude product was recrystallized from toluene and dried over molecular sieve.

A stoichiometric mixture of silver (0.470 g, 4.35 mmol, Chempur, 99.9%), tin (0.172 g, 1.45 mmol, Heraeus, 99.999%), copper (0.092 g, 1.45 mmol, Chempur, 99.999%), and red phosphorus (0.449 g, 14.5 mmol, Chempur, 99.999+%) was sealed in an evacuated silica ampule together with tin iodide (20 mg, 0.03 mmol) as a mineralizing agent. The mixture was slowly heated to 823 K within 3 h, kept at this temperature for 5 days, and then slowly cooled to room temperature. The crude product was homogenized and annealed at 823 K for 2 weeks, followed by slow cooling to ambient temperature. Traces of γ-AgI and SnI_4 were removed by washing with concentrated, aqueous ammonia solution and hot toluene. Single crystals of Ag_3SnCuP_{10} (**1**) suitable for X-ray structure determination were isolated from the bulk phase.

Cu_4SnP_{10} (**2**) and Ag_3SnP_7 (**3**) were prepared by reacting copper and red phosphorus in a tin flux or silver, tin, and red phosphorus plus additional tin(IV) iodide, as described in the literature.[4,6]

X-ray Powder and Single-Crystal Diffraction. Phase analysis was performed through X-ray powder patterns. A Stoe StadiP diffractometer was operated with Cu Kα radiation (λ = 1.54051 Å), and silicon was used as an external standard. Powder patterns prepared from the bulk phases proved the phase purity of Ag_3SnCuP_{10}. According to the reported preparation method, Cu_4SnP_{10} was always accompanied by small amounts of CuP_2. Nevertheless, single crystals for X-ray structure determination and Mössbauer spectroscopy could be separated from the bulk phase. Lattice parameters of (**1**) a = 10.503(1) and (**2**) a = 10.252(1) Å were found for both cubic materials. Single-crystal structure determinations were made on the basis of those values.

Single-crystal data of (**1**) were measured on an IPDS II (Stoe & Cie) in oscillation mode. Data for (**2**) were recorded on a four circle CAD4 (Nonius) diffractometer using $\omega/2\theta$ scans. Both systems were operated with graphite-monochromated Mo Kα radiation. A numerical absorption correction was applied to the data after optimization of the crystal shape from symmetry-equivalent reflections or Ψ scans, respectively.[13] A structure model related to (**2**) in space group $F\bar{4}3m$ (No. 216), a = 10.503(1) Å, was chosen after the structure solution for (**1**) with one mixed occupied 16*e* silver/tin, one 4*a* copper site, and two phosphorus positions on 16*e* and 24*g*. According to the quantitative analysis and in agreement with the structure model of (**2**), we applied a 0.25 tin and 0.75 silver mixing to the 16*e* position.

Single-crystal data of (**2**) were collected up to a diffraction angle of θ = 35.84°, and the crystal structure was redetermined in order to analyze the postulated mobility of copper on the 16*e* site of the $F\bar{4}3m$ model reported by W. Hönle and H. G. von Schnering.[4] A harmonic refinement of five independent positions using 279 reflections and 19 parameters resulted in final R values of R = 0.0227 and wR = 0.0412 for all reflections after absorption and extinction corrections. This model could not be improved by the introduction of nonharmonic terms. Occupancy factors of 0.25(1) and 0.75(1) were found after an unrestricted refinement of the tin/copper split sites.

NMR Spectroscopy. ^{31}P and ^{63}Cu NMR spectra were recorded at resonance frequencies of 202.5 (^{31}P) and 132.6 MHz (^{63}Cu) on a Bruker DSX-500 spectrometer. Solid state ^{31}P MAS NMR data were obtained on a 2.5 mm probe operating at spinning frequencies greater than 20 kHz; ^{63}Cu MAS NMR spectra were measured on a 4 mm probe at a frequency of 15 kHz. Typical acquisition parameters were pulse length 4.0 μs (90°) for ^{31}P and 1.0 μs (30°) for ^{63}Cu, recycle delay 150 s (^{31}P) and 2 s (^{63}Cu), number of scans 256 (^{31}P) and 1024 (^{63}Cu). Chemical shifts are referenced to crystalline CuI and 85% H_3PO_4, respectively.

To probe for the presence and strength of the heteronuclear dipole−dipole couplings, we conducted ^{63}Cu{^{31}P} rotational echo double resonance (REDOR)[14] and ^{31}P{^{63}Cu} rotational echo adiabatic passage double resonance (REAPDOR)[15] experiments in a 4 mm Bruker ^{31}P−X double-resonance probe in a 11.7 T magnet at spinning frequencies between 12 and 15 kHz. To correct the effects of small pulse imperfections, we used a formerly used compensation scheme described by J. C. C. Chan and H. Eckert in ^{63}Cu{^{31}P} REDOR experiments.[16] We accumulated 1024 transients for each measurement with a relaxation delay of 2 s, using 90° pulse lengths of 3 μs for ^{63}Cu and ^{31}P. ^{31}P{^{63}Cu} REAPDOR

(8) Bichat, M.-P.; Pascal, J.-L.; Gillot, F.; Favier, F. *Chem. Mater.* **2005**, *17*, 6761−6771.
(9) Vaughey, J. T.; Kepler, K. D.; Benedek, R.; Thackeray, M. M. *Electrochem. Commun.* **1999**, *1*, 517−521.
(10) Idota, Y.; Kubota, T.; Matsufuji, A.; Maekawa, Y.; Miyasaka, T. *Science* **1997**, *276*, 1395−1397.
(11) (a) Kozicki, M. N.; Mitkova, M.; Park, M.; Balakrishnan, M.; Gopalan, C. *Superlattices Microstruct.* **2003**, *34*, 459−465. (b) Pinnow, C.-U.; Happ, T. (Infineon Technologies AG, Germany) Patent DE 1020040-14965. (c) Pinnow, C.-U.; Mikolajick, T.; Happ, T.; Symanczyk, R. (Infineon Technologies AG, Germany) Patent DE 10323414.
(12) Brauer, G. *Handbuch der Präparativen Anorganischen Chemie*, 3rd ed.; F. Enke Verlag: Stuttgart, Germany, 1978; Vol. 2, p 759.
(13) (a) *X-RED 32*, version 1.10; Stoe & Cie GmbH: Darmstadt, Germany, 2004. (b) *X-SHAPE*, version 2.05; Stoe & Cie GmbH: Darmstadt, Germany, 2004.
(14) (a) Gullion, T.; Schäfer, J. *J. Magn. Reson.* **1989**, *81*, 196−200. (b) Gullion, T. *Magn. Reson. Rev.* **1997**, *17*, 83−131. (c) Bertmer, M.; Eckert, H. *Solid State Nucl. Magn. Reson.* **1999**, *15*, 139−159.
(15) (a) Gullion, T. *J. Magn. Reson.* **1995**, *A117*, 326−329. (b) Chopin, L.; Vega, S.; Gullion, T. *J. Am. Chem. Soc.* **1998**, *120*, 4406−4409.
(16) Chan, J. C. C.; Eckert, H. *J. Magn. Reson.* **2000**, *147*, 170−178.

measurements were conducted at a spinning speed of 15 kHz, using radio frequency amplitudes corresponding to nutation frequencies of 50 kHz for both ^{31}P and ^{63}Cu. The width of the adiabatic-passage pulse was set to 20 μs. We accumulated 512 transients with a relaxation delay of 100 s.

Mössbauer Spectroscopy. A $Ca^{119m}SnO_3$ source was available for the ^{119}Sn investigations, and a palladium foil of 0.05 mm thickness was used to reduce the tin K X-rays concurrently emitted by this source. The measurements were performed at 78 K and at room temperature in the usual transmission geometry. The samples were placed in thin-walled PVC containers to give a thickness between 10 and 15 mg of Sn per cm^2. A very small impurity of tetravalent tin was found for two materials, indicating the presence of oxidized species. No signals attributable to the mineralization agent SnI_4 (isomer shift of 1.52 mm s^{-1}) or binary phosphides such as SnP (isomer shift of 2.7 mm s^{-1}) and Sn_4P_3 (isomer shift of 2.9 mm s^{-1}) were observable.[17]

Electron Microprobe Analyses. Semiquantitative analysis was performed with a Leica 420i scanning electron microscope (Zeiss) fitted with an electron dispersive detector unit (Oxford). Cu, Ag, Sn, and GaP were used as standards for calibration; voltage = 20 kV. Ten independent measurements resulted in an averaged composition of $Ag_{2.8(1)}Sn_{1.00(2)}Cu_{1.0(1)}P_{10.0(1)}$. Iodine introduced to the reaction batch by the mineralization agent SnI_4 was not detected in any crystal.

Results and Discussion

Single-Crystal X-ray Structure Determination. Ag_3SnCuP_{10} (**1**), a new silver copper tin phosphide, combines the two almost-unique structural elements of $[Ag_3Sn]$ heteroclusters and $[P_{10}]$ cages (Figure 1a). The crystal structure was determined from single-crystal data.[18] A summary of selected crystallographic data and selected bond distances are given in Tables 1−3. Because of a possible symmetry reduction, discussed later in more detail, an orientationally ordered representation of the Ag_3Sn clusters (Figure 1b) is also shown instead of the disordered case in Figure 1a. A nonresolved Ag/Sn heteroclusters split position due to almost-identical Ag−P and Sn−P bond distances and an orientation disorder of the clusters are characteristic structural features that both demand a combination of state-of-the-art structure determination methods to get a reliable description of the crystal structure (Figure 2).

From a topological point of view, the structure of (**1**) can be derived from ternary tetrahedral structures of the zinc blende type. Copper builds up a face centered cubic (fcc) substructure. The $[Ag_3Sn]$ heteroclusters are arranged around the octahedral voids of the copper substructure. One-half of the tetrahedral voids are equivalent to the centers of gravity of the $[P_{10}]$ cages. A discussion of the crystal structure of (**2**) is reported in the literature; only a short summary will be given here.[4]

The decaphospha adamantane-type cage is a monomeric structural motif beside the well-characterized $[P_7]^{3-}$ and

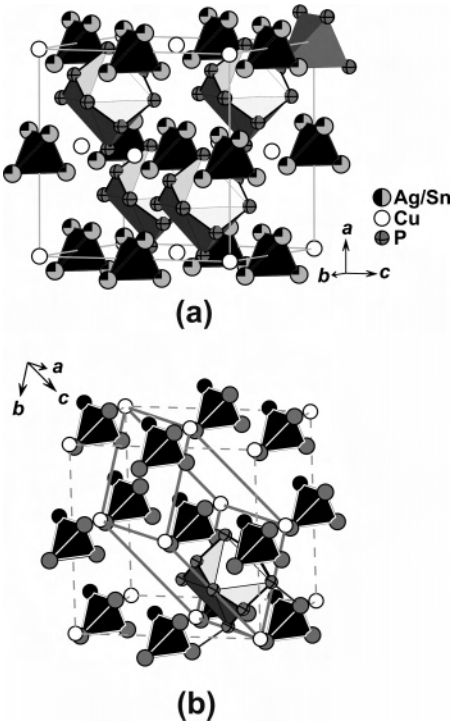

Figure 1. Crystal structure of Ag_3SnCuP_{10} (**1**). Copper builds up a fcc substructure with $[Ag_3Sn]$ heteroclusters (black polyhedra) arranged around all octahedral and adamantane-type $[P_{10}]$ cages around one-half of the tetrahedral voids. (a) Sectors representing a 25:75 Sn:Ag mixing in the $F\bar{4}3m$ model. One CuP_4 tetrahedron (grey polyhedron) is drawn for clarity. (b) Ordered orientation of the $[Ag_3Sn]$ heterocluster in the $R3m$ model. Only one $[P_{10}]$ cage is drawn for clarity. According to this model, an ideal 4-fold twin with $F43m$ pseudosymmetry may result.

$[P_{11}]^{3-}$ cages.[1] A bond distance of d(P−P) = 2.192(1) Å for the $[P_{10}]^{6-}$ cage in Ag_3SnCuP_{10} is a typical value reported for cage-type polyphosphides. Compared with that of the $[P_7]^{3-}$ cage (d(P−P) = 2.122(5)−2.288(5) Å in $Cs_3P_7 \cdot 3NH_3$ [19]) or the $[P_{11}]^{3-}$ cage (d(P−P) = 2.157−2.253 Å in $Cs_3P_{11} \cdot 3NH_3$ [20] or d(P−P) = 2.148−2.247 Å in $BaCsP_{11} \cdot 11NH_3$ [21]), the P−P bond distance is within the expected range. Two interesting geometrical counterparts of adamantane-type anions with four additional N atoms can be found with the $[P_4N_{10}]^{10-}$ cage embedded in a lithium matrix in $Li_{10}P_4N_{10}$ [22] or with the $[P_4(NH)_6N_4]^{4-}$ cage in $Na_{10}(NH_3)_{0.5}[P_4(NH)_6N_4](NH_2)_6$.[23]

The formulation of the $[Ag_3Sn]$ cluster is on the basis of results from semiquantitative EDX analyses and the assumption of monovalent silver, divalent tin cations, and hexavalent $[P_{10}]$ anions in (**1**). The oxidation state of tin was verified independently by ^{119}Sn Mössbauer spectroscopy (see Mössbauer spectroscopy section). The phase-pure preparation of (**1**) in combination with the occurrence of tetrahedrally coordinated copper substantiates the postulated oxidation states. Each of the sites within the cluster has a distorted

(17) (a) Flinn P. A. *Mössbauer Isomer Shifts*; Shenoy, G. K., Wagner F. E., Eds.; North-Holland Publishing Company: Amsterdam, 1978: pp 595−616. (b) Stevens, J. G.; Goforth, M. A. *^{119}Sn Mössbauer Spectroscopy*; Mössbauer Effect Data Centre: Ashville, NC, 1993.
(18) Sheldrick, G. M. *SHELXS-97, Program for Crystal Structure Solution*; University of Göttingen: Göttingen, Germany, 1997.
(19) Korber, N.; Daniels, J. *Helv. Chim. Acta* **1996**, *79*, 2083−2087.
(20) Knettel, D.; Reil, M.; Korber, N. *Z. Naturforsch., B: Chem. Sci.* **2001**, *56*, 965−969.
(21) Korber, N.; Daniels, J. *Z. Anorg. Allg. Chem.* **1996**, *622*, 1833−1838.
(22) Schnick, W.; Berger, U. *Angew. Chem.* **1991**, *103*, 857−858; *Angew. Chem., Int. Ed.* **1991**, *30*, 830−831.
(23) Jacobs, H.; Pollok, S.; Golinski, F. *Z. Anorg. Allg. Chem.* **1994**, *620*, 1213−1218.

Table 1. Selected Crystallographic Data for Ag_3SnCuP_{10} (**1**) and Cu_4SnP_{10} (**2**)[a]

	(**1**)	(**2**)
fw (g mol^{-1})	815.6	682.6
color	dark gray	dark gray
cryst habit	isomorphic	isomorphic
size (mm^3)	0.14 × 0.13 × 0.11	0.2 × 0.15 × 0.14
lattice parameter a (Å)	10.503(1)	10.252(1)
V (Å^3)	1158.0(6)	1077.6(1)
Z	4	
space group	$F\bar{4}3m$ (No. 216)	
T (K)	293(1)	
ρ_{calcd} (g cm^{-3})	4.68	4.21
no. of reflns	4333	2456
max.θ (deg)	34.75	34.87
diffractometer type	IPDS II	CAD 4
radiation, wavelength λ (Å)	MoKα radiation, 0.71073	
abs corr	numerical, optimized crystal shape	
μ (mm$-$1)	10.24	11.48
min./max. transmission	0.293/0.343	0.264/0.361
no. of independent reflns	256	279
R_{int}	0.0648	0.0300
structure solution; refinement	direct methods [18]; full matrix least-squares refinement on F^2 [28]	
no. of params	14	19
R1 ($I > 3\sigma(I)$)	0.0246	0.0213
wR2 ($I > 3\sigma(I)$)	0.0373	0.0408
R1 (all)	0.0278	0.0227
wR2 (all)	0.0377	0.0412
Δ ρ min./max. (e Å^{-3})	1.34/−0.83	1.59/−0.87
BASF	0.48(6)	0.01(2)

[a] Further details on the crystal structure investigations can be obtained from the Fachinformationzentrum Karlsruhe, 76344 Eggenstein-Leopoldshafen, Germany (fax: (49) 7247-808-666; E-mail: crysdata@fiz-karlsruhe.de) on quoting the depository numbers CSD 415695 (Ag_3SnCuP_{10}) and CSD 415696 (Cu_4SnP_{10}) and via the Internet at http://pubs.acs.org.

Table 2. Atomic Coordinates and Isotropic Displacement Parameters (Å^2) of (**1**) and (**2**)

atom	Wyckhoff	sof	x	y	z	U_{iso}
			(**1**)			
Cu	4*a*	1	0	0	0	0.0053(2)
Ag1	16*e*	0.75	0.09757(5)	x	$^1/_2 + x$	0.0207(1)
Sn1	16*e*	0.25	0.09757	x	$^1/_2 + x$	0.0207
P1	16*e*	1	0.1291(1)	x	x	0.0106(3)
P2	24*g*	1	0.0095(2)	$^1/_4$	$^1/_4$	0.0109(3)
			(**2**)			
Cu1	4*a*	1	0	0	0	0.0062(1)
Cu2	16*e*	0.75(1)	0.11980(5)	x	$^1/_2 - x$	0.0179(2)
Sn2	16*e*	0.25(1)	0.07519(6)	x	$^1/_2 - x$	0.0094(1)
P1	16*e*	1	0.12734(4)	$-x$	x	0.0058(1)
P2	24*g*	1	−0.0046(1)	$^1/_4$	$^1/_4$	0.0067(1)

Table 3. Selected Distances (Å) of (**1**) and (**2**)

(**1**)		(**2**)	
bond	length	bond	length
Cu1−P1	2.348(1)	Cu1−P1	2.261(1)
Ag1/Sn1− Ag1/Sn1	2.899(1)	Cu2−Sn2	2.864(1)
Ag1/Sn1−P2	2.528(1)	Cu2−P2	2.278(1)
		Sn2−P2	2.663(1)
P1−P2	2.192(2)	P1−P2	2.179(1)

trigonal-antiprismatic coordination of three phosphorus and three silver/tin atoms. Tin shows the typical coordination behavior of a system with lone-pair configuration, which can be found in other compounds such as tetrahedrites or thiometalates like $(MI)_2M_3SbS_3$ (M = Cu, Ag).[24] The bond distances of d(Sn−Ag) = d(Ag−Ag) = 2.899(1) Å are significantly smaller in (**1**) compared with cation−cation distances in other tetrahedral structures (d > 3.6 Å).[25] In

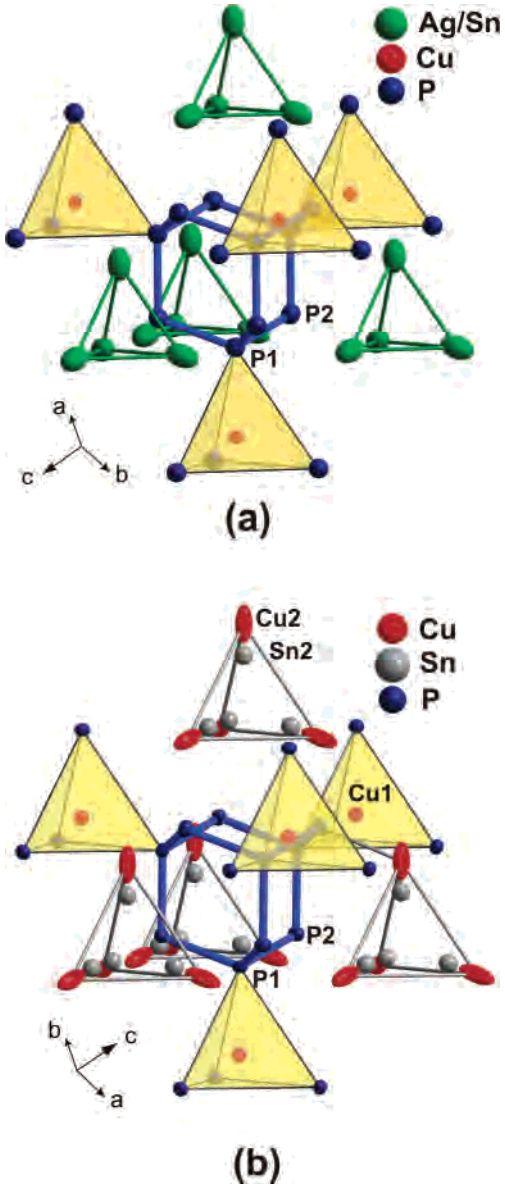

Figure 2. Positional and orientational disorder of M_3Sn heteroclusters in (a) Ag_3SnCuP_{10} (**1**), M = Ag and (b) Cu_4SnP_{10} (**2**), M = Cu. Coordination polyhedra are drawn for the heteroclusters (open polyhedra) and the tetrahedrally coordinated copper positions (colored polyhedra) in both compounds. Displacement parameters are at the 90% probability level.

relation to the sum of covalent radii (2.74 Å) and atomic radii (2.85 Å) of silver and tin, those distances suggest a metal−metal interaction within the $[Ag_3Sn]$ unit. A two-electron, four-center cluster results in an electron count of one negative charge per phosphorus atom with two homonuclear P−P bonds ($[P_{10}]^{6-}$), monovalent silver and divalent tin. Compared to those of (**2**) and (**3**), the P−Sn−P bond angles in the $[SnP_3]$ trigonal pyramid are significantly increased in (**1**), suggesting a more-pronounced sp^3 character in this compound (Table 4). To verify this situation from a

(24) (a) Wünsch, J. B. *Z. Kristallogr.* **1964**, *119*, 437−453. (b) Pfitzner, A.; Evain, M.; Petricek, V. *Acta Crystallogr., Sect. B* **1997**, *53*, 337−345. (c) Pfitzner, A. *Chem.−Eur. J.* **1997**, *3*, 2032−2038. (d) Nilges, T.; Reiser, S.; Hong, J. H.; Gaudin, E.; Pfitzner, A. *Phys. Chem. Chem. Phys.* **2002**, *4*, 5888−5894.

(25) (a) Gerlach, W. *Z. Kristallogr.* **1924**, *60*, 379−413. (b) Pfitzner, A.; Bernert, T. *Z. Kristallogr.* **2004**, *219*, 20−26.

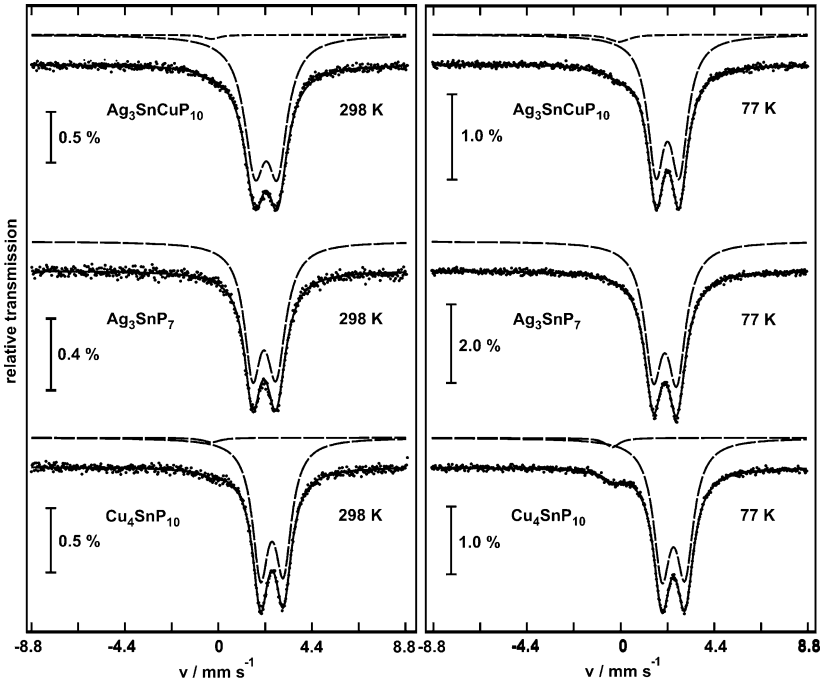

Figure 3. Experimental (points) and fitted (lines) ^{119}Sn Mössbauer spectra of (a) Ag_3SnCuP_{10} (**1**), (b) Ag_3SnP_7 (**3**), and (c) Cu_4SnP_{10} (**2**) at 298 and 77 K. The dashed lines represent the different signals fitted to the Mössbauer curves. The small signal at approximately 0 mm s^{-1} is due to traces of oxidized material in the samples.

Table 4. Distances (Å) and Angles (deg) of Trigonal Antiprismatically Coordinated Sn in M_3SnP_3 Units of (**1**), (**2**), and (**3**)

compound	d(M−Sn) (Å)	d(P−Sn) (Å)	∠(P−Sn−P) (deg)	reference
(**1**)	3 × 2.899(1)	3 × 2.528(1)	3 × 99.33(2)	this work
(**2**)	3 × 2.873	3 × 2.664	3 × 87.61	4
	3 × 2.864(1)	3 × 2.663(1)	3 × 87.72(2)	this work
(**3**)	2.834	2 × 2.587	85.50	6
	2 × 2.851	2.622	2 × 94.34	

theoretical point of view, we are currently performing band structure calculations.

A nonharmonic treatment[26] and an analysis of the resulting probability density functions[27] of the silver and copper heterocluster positions was performed to analyze the ion dynamics in (**1**) and the postulated one in (**2**). The presence of an enhanced ion dynamic should result in a nonharmonicity of the silver displacements toward neighbored cluster atoms, which could not be observed. A postulated mobility of copper or silver in (**2**) and (**1**) could not be found after a detailed examination of higher-order displacement parameters.[28] Details concerning the nonharmonic structure refinement and a comment on the crystallographic aspects can be found in the Supporting Information.

Mössbauer Data of Ag_3SnCuP_{10}, Ag_3SnP_7, and Cu_4SnP_{10} Cluster Compounds. The possibility of mutual Ag^+/Sn^{2+} disordering in the heterocluster needs to be discussed, because the latter has been observed for numerous silver/tin compounds (e.g., Ag_3SnI_5 [29]). Because the X-ray diffraction data cannot distinguish between a structure based exclusively on Ag_3Sn clusters and one bearing a statistical distribution of $Ag_{4-x}Sn_x$ clusters, a local probe is needed. To this end, ^{119}Sn Mössbauer spectra of (**1**), (**2**), and (**3**) were measured in order to get reliable information on the substitution-disorder situation in the comparable cluster compounds. For (**3**) a completely ordered orientation of the heterocluster was postulated.

One quadrupolar split signal was observed for each compound (Figure 3). All signals could be fitted by a single quadrupolar doublet with a line width parameter close to the "natural line width" of 0.80 mm s^{-1} expected from the nuclear excited-state lifetime (Table 5). The isomer shifts near 2 mm s^{-1} are typical values observed for the divalent tin oxidation state in many intermetallic compounds.[30] Any Ag^+/Sn^{2+} disordering would produce multiple tin sites, which should lead to significant line broadening effects in the Mössbauer spectra, at variance with the experimental observation. Examples of broadened signals are $Eu_2Au_2Sn_5$ (five Sn sites, line width 1.0 mm s^{-1} at 40 K),[31] $Ca_2Pt_3Sn_5$ (four Sn sites, line width 1.0 mm s^{-1} at 298 K),[32] or $Yb_2Pt_3Sn_5$ (five Sn sites, 0.97 mm s^{-1} at 4 K).[33]

(26) (a) Kuhs, W. F. *Acta Crystallogr., Sect. A* **1992**, *48*, 80−98. (b) Willis, B. T. M. *Acta Crystallogr., Sect. A* **1969**, *25*, 227−300.
(27) (a) Bachmann, R.; Schulz, H. *Acta Crystallogr., Sect. A* **1984**, *40*, 668−675. (b) Zucker, U. H.; Schulz, H. *Acta Crystallogr., Sect. A* **1982**, *38*, 563−568.
(28) Petricek, V.; Dusek, M.; Palatinus, L. *The Crystallographic Computing System JANA2000*; Institute of Physics: Praha, Czech Republic, 2000.
(29) Hull, S.; Keen, D. A.; Bergastegui, P. *J. Phys.: Condens. Matter* **2002**, *14*, 13579−13596.
(30) (a) Pöttgen, R.; Arpe, P. E.; Felser, C.; Kussmann, D.; Müllmann, R.; Mosel, B. D.; Künnen, B.; Kotzyba, G. *J. Solid State Chem.* **1999**, *145*, 668−677. (b) Müllmann, R.; Ernet, U.; Mosel, B. D.; Eckert, H.; Kremer, R. K.; Hoffmann, R.-D.; Pöttgen, R. *J. Mater. Chem.* **2001**, *11*, 1133−1140. (c) Wu, Z.; Hoffmann, R.-D.; Johrendt, D.; Mosel, B. D.; Eckert, H.; Pöttgen, R. *J. Mater. Chem.* **2003**, *13*, 2561−2565.
(31) Kussmann, D.; Pöttgen, R.; Rodewald, U. C.; Rosenhahn, C.; Mosel, B.; Kotzyba, G.; Kühnen, B. *Z. Naturforsch., B: Chem. Sci.* **1999**, *54*, 1155−1164.

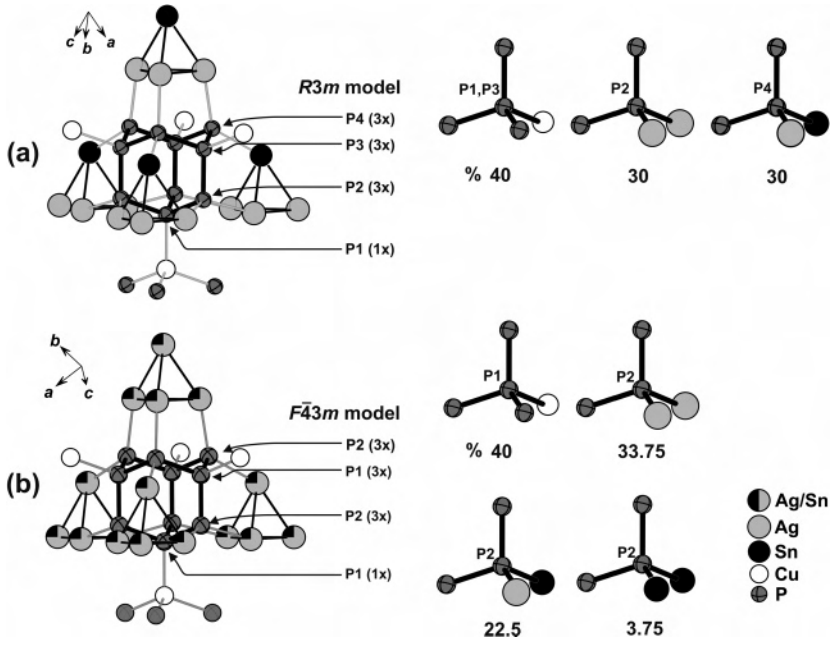

Figure 4. Two possible structure motifs of Ag_3SnCuP_{10} (**1**). (a) *R*3*m* model, featuring an ordered orientation of the [Ag_3Sn] heteroclusters. (b) A statistical distribution of silver and tin on the 16*e* position of the *F*43*m* model caused by a random orientation of the [Ag_3Sn] heterocluster. Right: Phosphorus coordination spheres for (**1**) according to the *F*$\bar{4}$3*m* (top right) and the *R*3*m* (bottom right) models. The distribution of the respective coordination type is given in percent.

Table 5. Fitting Parameters of ^{119}Sn Mössbauer Spectra of (**1**), (**2**), and (**3**) at 298 and 77 K

T (K)	δ (mm s^{-1})	ΔE_Q (mm s^{-1})	Γ (mm s^{-1})
	(**1**)		
298	−0.29(8)		0.76(2)
	2.03 (5)	0.97(4)	1.01(1)
77	−0.056(2)		1.04(1)
	2.03(4)	0.99(3)	0.88(1)
	(**2**)		
298	−0.30(9)		0.87(4)
	2.29 (4)	0.98(4)	0.84(1)
77	−0.29(2)		0.87(8)
	2.32(3)	0.99(3)	0.88(1)
	(**3**)		
298	1.94(8)	1.00(4)	0.99(1)
77	1.97(3)	1.01(3)	0.95(1)

δ, isomer shift; ΔE_Q, electric quadrupole interaction; Γ, experimental line width.

Mössbauer spectra of (**2**) show a slightly higher isomer shift compared to that of the title compound, which implies a somewhat different valence-electron hybridization with a higher s orbital contribution. The signals around 0 mm/s in (**1**) and (**2**) are caused by a very small impurity (<1%) of oxidized species.

Solid-State NMR Spectroscopy. To eliminate ambiguities in the structural description that arise from orientational (heteroclusters relative to the phosphide cage) and substitutional disorder (Ag/Cu and Ag/Sn mixing) effects, we found the use of local probes such as NMR spectroscopy to be essential. Both aspects will be discussed in combination of X-ray and solid-state NMR spectroscopic results.

The phosphorus atoms in (**1**) are four-coordinated by either three phosphorus and one copper atom or two phosphorus and two silver/tin atoms. Because the Ag−P and Sn−P bond distances are almost equal, two almost-identical structural scenarios can be formulated that differ only in the relative orientation of the [Ag_3Sn] clusters with respect to the P_{10} cage (see Figure 4). Random orientation generates a cubic *F*$\bar{4}$3*m* model with tin:silver 0.25:0.75 occupancy factors on the cluster position. In contrast, an ordered [Ag_3Sn] cluster arrangement results in a *R*3*m* model, with the clusters oriented in one direction only. Unfortunately, an ideal 4-fold domain crystal of oriented [Ag_3Sn] clusters ends up in exactly the same structure model and *F*$\bar{4}$3*m* pseudosymmetry. Thus, both scenarios are indistinguishable by single-crystal diffraction; the use of local probes is required for removing this ambiguity.[34]

Figure 4 demonstrates that both scenarios predict different distributions of local phosphorus environments. For the ordered model, three phosphorus sites in a 40:30:30 ratio are expected, whereas a statistical orientation of the [Ag_3Sn] heterocluster will produce four distinct phosphorus sites, including a [**P**P_2Sn_2] coordination polyhedron around the P2 position that is not present in the *R*3*m* model. Figure 5 shows the ^{31}P MAS NMR spectrum observed experimentally. As indicated by the spectral deconvolution using DIMFIT,[35] we observe four distinct spectral components at −149.3, −177.1, −191.7, and −220.0 ppm, with a relative area ratio of 22:42:31:5. This area ratio is consistent with a statistical distribution of silver and tin on the 16*e* position of the *F*$\bar{4}$3*m* model caused by a random orientation of the [Ag_3Sn]

(32) Hoffmann, R.-D.; Kussmann, D.; Rodewald, U. C.; Pöttgen, R.; Rosenhahn, C.; Mosel, B. D. *Z. Naturforsch., B: Chem. Sci.* **1999**, *54*, 709−717.
(33) Pöttgen, R.; Lang, A.; Hoffmann, R.-D.; Künnen, B.; Kotzyba, G.; Müllmann, R.; Mosel, B. D.; Rosenhahn, C. *Z. Kristallogr.* **1999**, *214*, 143−150.
(34) Bärnighausen, H. Personal communication, 2005.
(35) Massiot, D.; Fayon, F.; Capron, M.; King, I.; Le Calv, S.; Alonso, B.; Durand, J.-O.; Bujoli, B.; Gan, Z.; Hoatson, G. *Magn. Reson. Chem.* **2002**, *40*, 70−76.

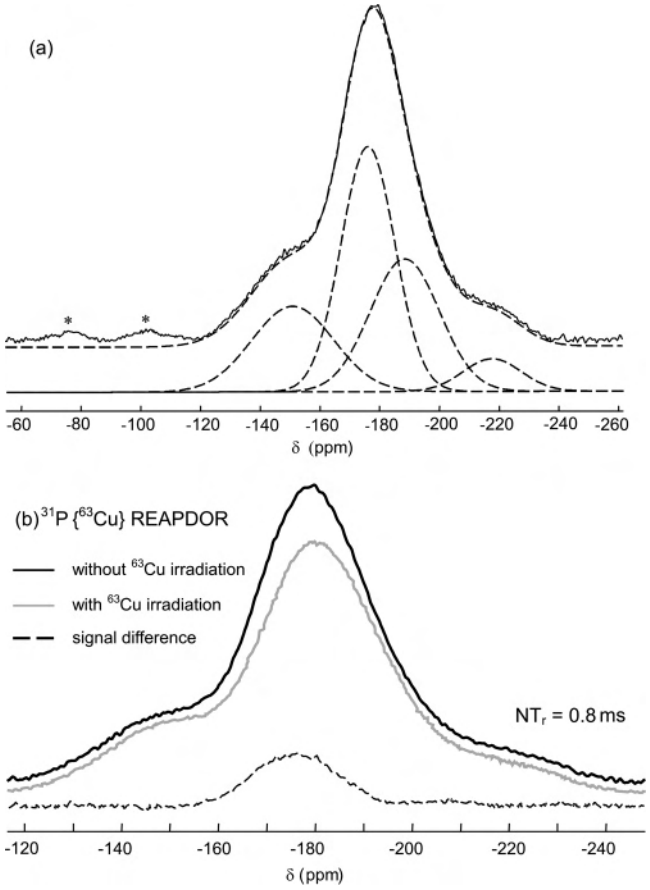

Figure 5. (a) ^{31}P MAS NMR spectrum (solid line) at 202.5 MHz of crystalline Ag_3SnCuP_{10} (**1**). Spectral deconvolution (dashed line) was made using DMFIT.[35] Spinning sidebands are indicated with asterisks. (b) ^{31}P{^{63}Cu} REAPDOR NMR carried out on (**1**). The upper and lower curves represent the ^{31}P signals without and with ^{63}Cu irradiation, respectively, during an evolution period of 0.8 ms. Also shown is the difference spectrum (dashed curve) of both curves. The line shape parameters of this difference spectrum are identical to those of the corresponding deconvolution component centered at −177.1 ppm in part (a) of the figure.

Table 6. ^{31}P Isotropic Chemical Shifts δ_{iso} and Relative Peak Area (RA) of Each Spectral Component in Crystalline (**1**), Determined via Spectral Deconvolution

	[**P**P$_3$Cu$_1$]	[**P**P$_2$Ag$_1$Sn$_1$]	[**P**P$_2$Ag$_2$]	[**P**P$_2$Sn$_2$]
δ_{iso} (ppm) (±0.5 ppm)	−177.1	−149.3	−191.7	−220.0
RA (%) exp (±1%)	42	22	31	5
RA (%) $F\bar{4}3m$ model	40	22.5	33.75	3.75
RA (%) $R3m$ model	40	30	30	

heterocluster. The assignment (summarized in Table 6) is supported further by ^{31}P{^{63}Cu} REAPDOR measurements. As shown in Figure 5b, only the signal assigned to [**P**P$_3$Cu$_1$] units at −177.1 ppm is attenuated by irradiation of the ^{63}Cu resonance during the rotor cycle, confirming that this phosphorus site is the only one having a direct P−Cu bond. On the basis of the corresponding difference spectrum seen in Figure 5b, we could selectively determine the width and position of this signal component, providing an important constraint for the overall ^{31}P NMR line shape fit given in Figure 5a. The fact that predominantly one phosphorus position only is affected by the REAPDOR experiment confirms that copper is ordered and that Cu/Ag mixing on the [Ag_3Sn] cluster sites does not occur to an appreciable extent. Such mixing, if it did occur, would then also produce

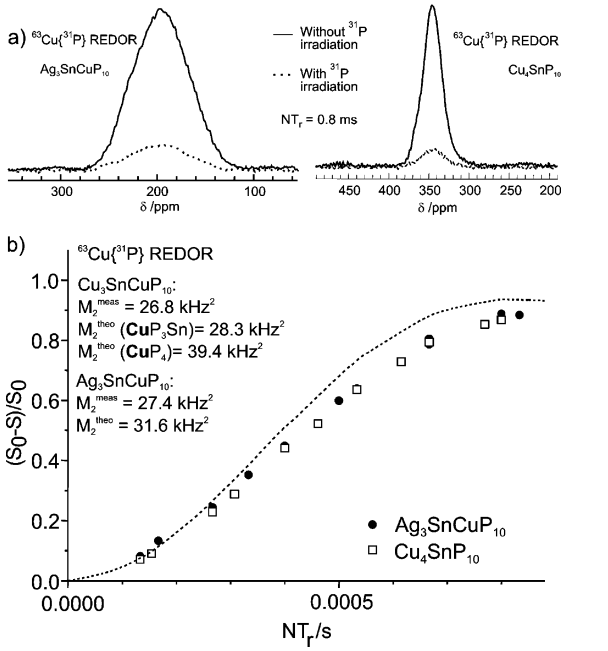

Figure 6. ^{63}Cu{^{31}P} REDOR experiments on Ag_3SnCuP_{10} (**1**) and Cu_4SnP_{10} (**2**). (a) ^{63}Cu spectra with and without ^{31}P irradiation during a dipolar evolution time of 0.8 ms for (**1**) (left) and (**2**) (right). (b) Plots of REDOR difference signal intensity vs dipolar evolution time and comparison with a simulated curve for a CuP_4 tetrahedron using the internuclear distance of 2.348 Å (**1**) and 2.261 Å (**2**) from the crystal structures. Experimental data for (**2**) measured at spinning speeds of 15 and 13 kHz are included for comparison (open squares). Experimental second moments (M_2 values) as obtained from an analysis of the initial curvatures ($0 \le \Delta S/S_0 \le 0.2$) (see ref 16) are compared with calculated values from crystal structural data.

REAPDOR effects on the other phosphorus resonances (which are not observed). The ^{31}P MAS NMR spectrum of reference compound (**2**) (see the Supporting Information, Figure S1) shows a similar intensity distribution, with four peaks at −108.4 (43%), −122 (23%), −92.5 (31%), and −74.6 ppm (3%). Because of the overall limited spectral resolution and the presence of substantial ^{31}P−^{63}Cu interactions for all line shape components, no straightforward fitting constraints are available. Nevertheless, a reasonable fit to the data can be achieved that is consistent with the intensity distribution predicted by the $F\bar{4}3m$ model. Tentative peak assignments made on this basis are listed in the Supporting Information. The chemical shifts measured for the different phosphorus sites in this compound are significantly different from those in (**1**), suggesting that nonlocal effects make a significant contribution to the chemical shifts in these materials. These nonlocal effects comprise contributions from unpaired conduction electron spin density near the Fermi level (Knight shifts), as frequently encountered in semiconducting and metallic compounds.

Figure 6 shows ^{63}Cu line shapes and ^{63}Cu{^{31}P} REDOR results on (**1**) (Figure 5a) and (**2**) (Figure 5b). For (**1**), the ^{63}Cu MAS NMR peak position (195 ± 5 ppm) and full width at half-maximum (9600 Hz) are found to be independent of the applied magnetic field strength at 11.7 and 4.7 T, suggesting that the main source of broadening is not attributable to second-order nuclear electric quadrupolar effects but rather to direct and indirect heteronuclear dipole−dipole interactions. Upon irradiation with ^{31}P π pulses during

the rotor period, the signal is attenuated appreciably, consistent with very strong heteronuclear dipole−dipole interactions, as expected. In the bottom part of Figure 6, the magnitude of the difference signal is plotted as a function of dipolar evolution time, recorded at two different spinning speeds. The data measured for (**1**) agree well with a simulation for a regular CuP_4 tetrahedron with a Cu−P distance of 234.8 pm. (the small deviations may come from the superimposed effect of indirect spin−spin interactions, which cannot be measured separately). The ^{63}Cu MAS NMR spectrum of (**2**) shows a relatively sharp ^{63}Cu NMR signal at 350 ppm. Compared to those of Ag_3SnCuP_{10}, the ^{31}P−^{63}Cu interactions are very similar in magnitude. This is expected from the crystal structure, which shows the four copper sites in CuP_4 tetrahedral and CuP_3Sn_3 trigonal antiprismatic environments (in a 1:3 ratio), with significantly shorter Cu−P distances (2.261−2.278 Å). Indeed, a calculation of the dipolar second moments characterizing the ^{63}Cu−^{31}P dipole−dipole couplings from the known internuclear distances produces nearly identical values (31.6×10^6 rad^2 s^{-2} vs 31.1×10^6 rad^2 s^{-2} for (**1**) and (**2**), respectively) for both compounds.

All these experiments support the absence of Ag/Cu mixing in the [Ag_3Sn] clusters in (**1**). Consistent with this conclusion, experimental attempts of preparing $Ag_{3-x}SnCu_{1+x}P_{10}$ ($x = 1, 2$) phases with mixed [$Ag_{3-x}Cu_xSn$] clusters or mixed occupancies of the Cu position were unsuccessful, yielding only mixtures of (**1**) and binary phases.

Conclusion

(**1**) is one representative of an interesting scientific field in solid-state chemistry that joins metal-cluster chemistry with polyphosphide-based cage compounds. The structural features of (**1**) consisting of [Ag_3Sn] heterocluster and adamantane-type P_{10} cages have been addressed by solid-state NMR techniques and single-crystal X-ray structure analysis. The coexistence of both structural units creates new forms of orientational and substitutional disorder that cannot be fully characterized by diffraction methods alone. (**1**) serves as an example in which a complete structure determination is possible only by the combined application of diffractometry and spectroscopy.

Acknowledgment. This paper is dedicated to Prof. Dr. H. G. von Schnering on the occasion of his 75th birthday.The NMR results were supported by DFG Grant Ec168/7-1; and C.P.S. is funded by the NRW Graduate School of Chemistry.

Supporting Information Available: CIF files of Ag_3SnCuP_{10} and Cu_4SnP_{10}, comments on the ion dynamic in Ag_3SnCuP_{10}, ^{31}P MAS NMR spectrum of Cu_4SnP_{10}, listing of the ^{31}P isotropic chemical shifts. This material is available free of charge via the Internet at http://pubs.acs.org.

IC060380A